

Bilayer graphene Origami: curvature-induced p-n junctions

Yogesh N. Joglekar

Department of Physics, Indiana University-Purdue University Indianapolis (IUPUI), Indianapolis, Indiana 46202, USA

Avadh Saxena

Theoretical Division, Los Alamos National Laboratory, Los Alamos, New Mexico 87545, USA

(Dated: September 27, 2018)

A massive quantum particle on a two-dimensional curved surface experiences a surface-geometry induced attractive potential that is characterized by the radii of curvature at a given point. With bilayer graphene sheets and carbon nano-ribbons in mind, we obtain the geometric potential V_G for several surface shapes. Under appropriate conditions that we discuss in detail, this potential suppresses the local Fermi energy. Therefore, we argue that in zero band-gap materials with a quadratic band structure, it will create p- and n-type regions. We discuss the consequences of this result, and suggest that surface curvature can provide a novel avenue to create p-n junctions and, in general, to control local electronic properties in carbon nano-ribbons and bilayer graphene sheets.

PACS numbers: 72.80.Rj, 02.40.-k, 71.10.Pm

Introduction: The classical dynamics of a particle subject to (holonomic or non-holonomic) constraints is well-understood. In Lagrangian formulation, these constraints can be represented by an effective potential.¹ In quantum theory, the potential representing constraints plays an instrumental role in determining the quantized spectrum of the system.² Indeed, low-dimensional systems are realized by constraints that classically restrict the motion of the particle in one or more directions. For example, in two-dimensional electron (or hole) systems (2DES), typically realized in III-V semiconductor heterojunctions³ the barrier potential at the heterojunction interface, created by differing electron affinities, leads to a clear separation of energy scales for the motion in the 2D plane and motion along the direction normal to the plane. It allows one to separate the particle wavefunction into normal and surface components and, at low energies, focus solely on the surface component.⁴

The quantum properties of a non-relativistic particle constrained⁵ on an arbitrary orientable surface were first investigated by da Costa.^{6,7} He showed that apart from the necessity of expressing the Laplace-Beltrami operator ∇^2 in terms of the curvilinear surface co-ordinates, the geometry of the surface also leads to an attractive geometric potential $V_G(q_1, q_2) = -(\hbar^2/8m)(\kappa_1 - \kappa_2)^2$ where m is the mass of the particle, (q_1, q_2) denote surface co-ordinates, and κ_1, κ_2 are the two position-dependent principal curvatures of the surface. Note that this potential is purely a result of particle confinement, and therefore is independent of the electric charge of the particle; it is therefore the same for electrons and holes. This result is applicable in the limit $W\kappa \rightarrow 0$ where W is the thickness of the “two-dimensional” surface and κ is the surface curvature. W will correspond to the width of the quantum well in 2DES. The geometric potential is small near a surface maximum or minimum, and is large near saddle regions where $\kappa_1\kappa_2 < 0$. In particular, we note that for surfaces with a constant curvature (spherical sections or a plane) the geometric potential is equal to zero,

$V_G = 0$. The bound states that appear due to the geometric potential⁸ and the resultant resonance microwave absorption⁹ have been investigated in twisted¹⁰ or bent (quasi one-dimensional electron) waveguides.¹¹ The effect of curvature on spin-orbit coupling has been studied in the case of nanospheres and nanotubes.¹² More recently, the geometric-potential induced charge separation in helicoidal ribbons has been analytically explored.¹³ However, absent a truly two dimensional system that can be (easily) bent, the effect of geometric potential on the electronic band structure has been justifiably ignored.

In this paper, we point out that the geometric potential provides a hitherto unexplored avenue to locally change the carrier polarity in zero-gap materials. We predict that it will be possible to create p-n or n-p-n junctions purely from a suitable surface geometry. Bilayer graphene provides an ideal realization of a zero-gap material with chiral electrons and holes that have identical mass. Graphene nano-ribbons (GNR), recently created by unzipping single and multi-walled carbon nanotubes¹⁴ may provide another promising candidate that can be used to explore the curvature effects in a gapless semiconductor. Therefore, in this paper we primarily focus on bilayer graphene. In the next section, we obtain the geometric potential for two generic cases: first a surface $z = f(x)$ that is isometric to a plane and second a catenoid that is *not* isometric to a plane. In the following section, we show that at present carrier densities n_{2D} , carriers in bilayer graphene, with its Bernal-stacked hexagonal lattice structure, can be treated as massive particles on a curved surface. We conclude the paper with a qualitative discussion about experimental consequences and speculation regarding the geometric potential for monolayer graphene with massless chiral carriers.

Monolayer and bilayer graphene have been studied in great detail in recent years. P-N junctions in monolayer graphene are fabricated by local top-gating¹⁵ and with an air-bridge top gate.¹⁶ Bilayer graphene has been explored for its electric field tunability.^{17,18} The effect of

random surface curvature (ripples) on electronic properties in monolayer graphene is primarily described via gauge potentials¹⁹; however, the effect of geometric potential in monolayer and bilayer graphene has not been investigated. In *monolayer* graphene near the neutrality point, disorder induced electron-hole puddles and the resulting array of p-n junctions is observed.²⁰ However, in this case, the origin of the disorder and the role, if any, played by monolayer surface curvature is unclear.²⁰ In particular, the topic of p-n junctions made with bilayer graphene (that we propose in this paper) has been scarcely investigated.

In this paper, we argue that due to its essentially two-dimensional nature ($W\kappa \rightarrow 0$), gapless quadratic band structure, and exceptional material strength, bilayer graphene presents an excellent candidate for exploration of two-dimensional systems with curvature.

Continuum Model: Let us consider a non-relativistic particle of (effective) mass m constrained to a surface given by $z = f(x)$ (See Fig. 1). We characterize a point

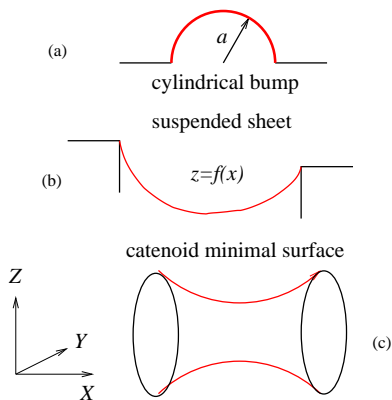


FIG. 1: (Color online) Schematic shapes of various curved surfaces considered in this paper. The top two, a sheet with a cylindrical bump with radius a (a) and a sheet suspended between two mesas (b), have only one nonzero principal curvature $\kappa(x)$ and are isometric to a plane. The surface at the bottom, a catenoid (c), has two nonzero principal curvatures at each point $\kappa_1(x, y)\kappa_2(x, y) < 0$.

on the two-dimensional surface embedded in the three-dimensional space by $\mathbf{r} = (x, y, f(x))$. The geometric potential is obtained from the two fundamental forms associated with the surface.⁶ The first fundamental form or, equivalently, the (diagonal) metric tensor²¹ for the surface is given by $g_{ij} = \partial_i \mathbf{r} \cdot \partial_j \mathbf{r} = \text{dia}(1 + f'^2(x), 1)$ where $i, j = x, y$ and $f' = df/dx$. The second fundamental form $h_{ij} = -\partial_i \mathbf{r} \cdot \partial_j \mathbf{n}$ characterizes the change in the surface-normal \mathbf{n} along the surface²¹ and has only one nonzero element, $h_{xx}(x) = -f''(x)/[1 + f'(x)^2]^{3/2}$ where $f'' = d^2f/dx^2$. Principal curvatures of the surface are eigenvalues of the matrix⁶ $\alpha = -hg^{-1}$ and, in this case, they are given by $\kappa_1(x) = f''(x)/\sqrt{1 + f'(x)^2}$ and $\kappa_2 = 0$. The zero eigenvalue reflects the translational invariance of the system in the y -direction, and the zero Gaussian curvature $K = \kappa_1\kappa_2 = 0$ everywhere on the

surface implies that it is isometric to a plane.²¹ Thus, for such a surface, the geometric potential is given by $V_G(x) = -(\hbar^2/8m)[f''(x)/\sqrt{1 + f'(x)^2}]^2$.

We remind the reader that the potential is purely quantum, can be different for isometric surfaces (for example, a plane and a cylinder), and is always attractive. The Hamiltonian for the constrained particle is $\hat{H} = \hat{H}_0 + \hat{V}_G$ and the kinetic contribution is given by

$$\hat{H}_0 = -\frac{\hbar^2}{2m} \frac{1}{\sqrt{g}} \partial_i [\sqrt{g}(g^{-1})_{ij} \partial_j] \quad (1)$$

$$= -\frac{\hbar^2}{2m} \left[\frac{d^2}{ds^2} + \frac{d^2}{dy^2} \right], \quad (2)$$

where $g = \det g_{ij}$, and $s(x) = \int_0^x du \sqrt{1 + f'(u)^2}$ is the arc-length along the surface. In terms of the surface coordinates (s, y) , the geometric potential term becomes

$$V_G(s(x), y) = -\frac{\hbar^2}{8m} \left[\frac{s'(x)}{s'(x)^2 \sqrt{s'(x)^2 - 1}} \right]^2. \quad (3)$$

Note that for a cylindrical bump of radius a (Fig. 1a), we recover⁶ a constant geometric potential $V_G = -\hbar^2/8ma^2$. This attractive geometric potential is independent of the sign of the curvature: a bump, a trough, or combinations thereof lead to the same constant attractive potential. For a suspended sheet (Fig. 1b),²² $f(x) = a[1 - \cosh(x/a)]$ where a sets the length-scale for the catenary, the geometric potential is given by

$$V_G(s(x), y) = -\frac{\hbar^2}{8ma^2} \left[\frac{a^2}{a^2 + s^2} \right]^2. \quad (4)$$

Lastly, we consider the particle confined to a catenoid (Fig. 1c) parameterized by two dimensionless surface co-ordinates (u, v) where $x = a \cosh(u) \cos(v)$, $y = a \cosh(u) \sin(v)$ and $z = au$. Note that perfect (bilayer) graphene sheets are planar and, as such, they cannot be mapped onto a surface with nonzero Gaussian curvature. However, fullerenes or dislocations in the honeycomb lattice can lead to surfaces with nonzero Gaussian curvature. A straightforward calculation gives the geometric potential

$$V_G(u, v) = -\frac{\hbar^2}{2ma^2} \frac{1}{\cosh^4(u)}. \quad (5)$$

We note that $V_G(u, v)$ is solely a function of u , just as $V_G(s, y)$ in Eq.(3) is solely a function of s . However, unlike in the former case, the kinetic energy term on the catenoid $\hat{H}_0 = -(\hbar^2\kappa_1(u)/2ma)(\partial^2/\partial u^2 + \partial^2/\partial v^2)$ is not separable and reflects the nonzero Gaussian curvature of the surface.

Applicability to Bilayer Graphene: To map a curved bilayer graphene sheet onto a quantum particle on a curved surface, two criteria must be satisfied: $k_F a_G \ll 1$ and $\kappa a_G \ll 1$ where $a_G = 1.4 \text{ \AA}$ is the carbon-carbon distance in graphene, k_F is the Fermi wavevector, and κ

is the surface curvature. The first criterion ensures that bilayer graphene can be treated in the continuum limit. In this limit, for carrier densities $n_{2D} \lesssim 3.5 \times 10^{13} \text{ cm}^{-2}$, only the gapless valence and conduction bands are occupied^{23,24} and the carriers can be approximated as particles with an effective mass $m^* \sim 0.03m_e$. The second criterion ensures the detailed lattice structure can be ignored on the curvature length-scale, and because the “thickness” of bilayer graphene sheets is $W \sim 3a_G$, it also ensures that $W\kappa \ll 1$, or that the bilayer graphene sheet with nonzero thickness can be considered a surface. The first criterion is easily satisfied at present carrier densities in bilayer graphene with $n_{2D} \sim 10^{12} \text{ cm}^{-2}$ and corresponding $k_F \sim 10^{-2} \text{ \AA}^{-1}$. The second criterion, $\kappa a_G \ll 1$ is satisfied by carbon nanotubes with typical radii $1/\kappa \sim 10\text{-}30 \text{ \AA}$ and by typical surface ripples on monolayer graphene.²⁵ When $\kappa \sim k_F$ the geometric potential V_G becomes comparable to the Fermi energy $E_F = \hbar^2 k_F^2 / 2m^*$, whereas in “planar” bilayer graphene $\kappa \approx 0 \ll k_F \ll 1/a_G$.

Within the continuum approximation, we can consider two cases. When $1/a_G \gg \kappa \gg k_F$ the problem is reduced to that of a single-particle in an attractive external potential.¹³ This case is not very realistic since at (vanishingly) low carrier densities, disorder effects dominate the physics.^{20,26} On the other hand, when $\kappa \sim k_F \ll 1/a_G$, the geometric potential will reduce the local Fermi energy. In particular, if we consider graphene with n-type carriers in the flat region ($E_{F0} > 0$), the geometric potential will lower the Fermi energy from the conduction band to the valence band, $E_F(q_1, q_2) = E_{F0} - |V_G(q_1, q_2)| < 0$. Note that as long as the geometric potential is constant or slowly varying (as would be the case for a cylindrical bump), this result is robust and is independent of any other quantum numbers, such as chirality or electric charge, that the carriers may have. Therefore, *we predict that in such a configuration, the curved regions will have p-type carriers with a natural p-n junction created between the curved and flat regions.* For the surface $z = f(x)$, the geometric potential will create p- and n-type strips where the location, size, and polarity of each strip is determined by the local Fermi energy $E_F(x)$.

Bilayer graphene is distinguished from its semiconductor counterparts by the chiral nature of its carriers that leads to zero transmission probability for normal incidence at a potential barrier in spite of the zero gap between the electron and hole bands.²⁷ Thus, the chirality of the carriers in bilayer graphene will only affect the transparency (i.e. the transmission amplitude as a function of incidence angle) of the p-n junctions created by the geometric potential.²⁸ Such p-n junctions can be created by either depositing bilayer graphene on a patterned substrate with requisite bumps and troughs with radii $R \sim 100 \text{ \AA}$ or by suspending it across a narrow channel. A local probe²⁹ may also offer an alternative

way to induce controlled curvature in a suspended bilayer graphene sheet. We emphasize that our prediction is valid for any two-dimensional zero-gap semiconductor with appropriate curvature, although bilayer graphene and GNRs are the most promising candidates.

Discussion: In this paper we have proposed that bilayer graphene on a patterned substrate provides a novel avenue to create a p-n junction. Our prediction provides a direct way to experimentally probe the effect of geometric potential that has been, hitherto, neglected in two-dimensional systems.

The origin of the geometric potential V_G is well-understood for a non-relativistic massive particle.⁶ In case of a planar 2DES, a lattice model naturally leads to carriers with an effective mass. However, a lattice-model generalization of the geometric potential is, to our knowledge, an open question. The primary difficulty in addressing such a question is that typical lattice models start with zero thickness, $W = 0$, whereas the geometric potential arises from taking the limit $W \rightarrow 0$.

We conclude the paper with speculation about curved monolayer graphene. Since the geometric potential V_G is obtained from non-relativistic Schrödinger equation, *prima facie* is not applicable to monolayer graphene where the carrier dynamics is well-described by the two-dimensional Dirac Hamiltonian. Monolayer graphene with random curvature (ripples) is modeled using random gauge fields¹⁹ and mean-curvature-dependent potential.³⁰ We are unaware of a rigorous derivation of geometric potential for massless particles or for a lattice-model that leads to linearly dispersing bands. Dimensional analysis implies that for a surface $z = f(x)$, the geometric potential, if nonzero, must scale as $V_G \propto \hbar v_G |\kappa|$ where v_G is the velocity of massless carriers in graphene.³¹ It follows that under the conditions discussed in the last section, this geometric potential will locally change the Fermi energy $E_F(x)$ and will lead to the formation of a p-n junction. We remind the reader that the transparency of such a junction in monolayer graphene is drastically different from that in bilayer graphene although both are zero-gap materials.²⁷

The test of our prediction via experiments and the generalization of the geometric potential to a lattice model will provide insights into the electronic structure of curved two-dimensional materials with zero band-gap. Curvature induced p-n and p-n-p junctions in bilayer graphene and the GNR may open up new vistas for nano-electronics.

Acknowledgments: Y.J. thanks Sasha Balatsky for the opportunity to visit Los Alamos National Laboratory and acknowledges the hospitality of KITP, Santa Barbara (Grant No. NSF PHY05-51164) during the completion of this work. This work was supported in part by the U.S. Department of Energy.

-
- ¹ H. Goldstein, C. Poole, and J. Safko, *Classical mechanics* (Addison Wesley, New York, 2002).
- ² D.J. Griffiths, *Introduction to quantum mechanics* (Benjamin Cummings, New York, 2004).
- ³ M. Sundaram, S.A. Chalmers, P.F. Hopkins, and A.C. Gossard, *Science* **254**, 1326 (1991).
- ⁴ T. Ando, A.B. Flower, and F. Stern, *Rev. Mod. Phys.* **54**, 437 (1982).
- ⁵ H. Jensen and H. Koppe, *Ann. Phys.* **63**, 586 (1971).
- ⁶ R.C.T. da Costa, *Phys. Rev. A* **23**, 1982 (1981).
- ⁷ The role of curvature in the spectrum of a particle confined between equidistant surfaces was explored in ref. 5.
- ⁸ J. Goldstone and R.L. Jaffe, *Phys. Rev. B* **45**, 14100 (1992).
- ⁹ J. Carini *et al.*, *Phys. Rev. B* **46**, 15538 (1992).
- ¹⁰ I.J. Clark and A.J. Bracken, *J. Phys. A* **29**, 339 (1996).
- ¹¹ G. Timp *et al.*, *Phys. Rev. Lett.* **60**, 2081 (1988).
- ¹² M.V. Entin and L.I. Magarill, *Phys. Rev. B* **64**, 085330 (2001).
- ¹³ V. Atanasov, R. Dandoloff, and A. Saxena, *Phys. Rev. B* **79**, 033404 (2009).
- ¹⁴ D.V. Kosynkin *et al.*, *Nature (London)* **458**, 872 (2009); L. Jiao *et al.*, *Nature (London)* **458**, 878 (2009).
- ¹⁵ J.R. Williams, L. DiCarlo, and C.M. Marcus, *Science* **317**, 638 (2007).
- ¹⁶ R.V. Gorbachev *et al.*, *Nano Lett.* **8**, 1995 (2008).
- ¹⁷ O. Taisuke, A. Bostwick, T. Seyller, K. Horn, and E. Rotenberg, *Science* **313**, 951 (2006).
- ¹⁸ J.B. Oostinga *et al.*, *Nat. Mat.* **7**, 151 (2008).
- ¹⁹ F. Guinea, B. Horovitz, and P. Le Doussal, *Phys. Rev. B* **77**, 205421 (2008).
- ²⁰ J. Martin *et al.*, *Nat. Phys.* **4**, 144 (2008).
- ²¹ W.A. Boothby, *An introduction to differentiable manifolds and Riemannian geometry* (Academic Press Inc., Boston, 1986).
- ²² Strictly speaking, this expression is true only for an infinite hanging sheet.
- ²³ E. McCann and V.I. Fal'ko, *Phys. Rev. Lett.* **96**, 086805 (2006).
- ²⁴ E.V. Castro *et al.*, *Phys. Rev. Lett.* **99**, 216802 (2007).
- ²⁵ F. Fasolino, J.H. Los, and M.I. Katsnelson, *Nat. Mat.* **6**, 858 (2007).
- ²⁶ J.-H. Chen *et al.*, *Nat. Phys.* **4**, 377 (2008).
- ²⁷ M.I. Katsnelson, K.S. Novoselov, and A.K. Geim, *Nat. Phys.* **2**, 620 (2006).
- ²⁸ Although the phenomenon of Klein tunneling across p-n junctions in *monolayer* graphene has been extensively explored,^{15,16,27} properties of p-n junctions in *bilayer* graphene are not as clear.
- ²⁹ I.W. Frank, D.M. Tanenbaum, A.M. van der Zande, and P.L. McEuen, *J. Vac. Sci. Technol. B* **25**, 2558 (2007).
- ³⁰ E.A. Kim and A.H. Castro Neto, *Euro. Phys. Lett.* **84**, 57007 (2008) and references therein.
- ³¹ M. Ouyang *et al.*, *Science* **292**, 702 (2001).